Journal of
Clinical Medicine

MDPI

Article

Metabolomic Alteration of Oral Keratinocytes and Fibroblasts in Hypoxia

Hiroko Kato [1,2,3,*], Masahiro Sugimoto [4,5], Ayame Enomoto [5], Miku Kaneko [5], Yuko Hara [2], Naoaki Saito [2], Aki Shiomi [6], Hisashi Ohnuki [2] and Kenji Izumi [2,*]

1 Research Center for Advanced Oral Science, School of Medical and Dental Sciences, Niigata University, Nii-gata 951-8514, Japan
2 Division of Biomimetics, School of Medical and Dental Sciences, Niigata University, Niigata 951-8514, Japan; hyuko@dent.niigata-u.ac.jp (Y.H.); nao-saito@dent.niigata-u.ac.jp (N.S.); oonuki.hisashi@maroon.plala.or.jp (H.O.)
3 Laboratory of Advanced Cosmetic Science, School of Pharmaceutical Sciences, Osaka University, Suita, Osaka 565-0871, Japan
4 Research and Development Center for Minimally Invasive Therapies, Health Promotion and Preemptive Medicine, Tokyo Medical University, Tokyo 160-8402, Japan; mshrsgmt@tokyo-med.ac.jp
5 Institute for Advanced Biosciences, Keio University, Tsuruoka, Yamagata 997-0052, Japan; ayame.e@ttck.keio.ac.jp (A.E.); kkk-miku@ttck.keio.ac.jp (M.K.)
6 Division of Dental Education Research Development, School of Medical and Dental Sciences, Niigata University, Niigata 951-8514, Japan; as.aki.mh@gmail.com
* Correspondence: kato-hi@phs.osaka-u.ac.jp (H.K.); izumik@dent.niigata-u.ac.jp (K.I.); Tel.: +81-6-6105-5792 (H.K.); +81-25-227-2850 (K.I.); Fax: +81-6-6105-5790 (H.K.); +81-25-227-2854 (K.I.)

Citation: Kato, H.; Sugimoto, M.; Enomoto, A.; Kaneko, M.; Hara, Y.; Saito, N.; Shiomi, A.; Ohnuki, H.; Izumi, K. Metabolomic Alteration of Oral Keratinocytes and Fibroblasts in Hypoxia. *J. Clin. Med.* **2021**, *10*, 1156. https://doi.org/10.3390/jcm10061156

Academic Editor: Ryou-u Takahashi

Received: 6 February 2021
Accepted: 2 March 2021
Published: 10 March 2021

Abstract: The oxygen concentration in normal human tissue under physiologic conditions is lower than the atmospheric oxygen concentration. The more hypoxic condition has been observed in the cells with wound healing and cancer. Somatic stem cells reside in a hypoxic microenvironment in vivo and prefer hypoxic culture conditions in vitro. Oral mucosa contains tissue-specific stem cells, which is an excellent tissue source for regenerative medicine. For clinical usage, maintaining the stem cell in cultured cells is important. We previously reported that hypoxic culture conditions maintained primary oral keratinocytes in an undifferentiated and quiescent state and enhanced their clonogenicity. However, the metabolic mechanism of these cells is unclear. Stem cell biological and pathological findings have shown that metabolic reprogramming is important in hypoxic culture conditions, but there has been no report on oral mucosal keratinocytes and fibroblasts. Herein, we conducted metabolomic analyses of oral mucosal keratinocytes and fibroblasts under hypoxic conditions. Hypoxic oral keratinocytes and fibroblasts showed a drastic change of metabolite concentrations in urea cycle metabolites and polyamine pathways. The changes of metabolic profiles in glycolysis and the pentose phosphate pathway under hypoxic conditions in the oral keratinocytes were consistent with those of other somatic stem cells. The metabolic profiles in oral fibroblasts showed only little changes in any pathway under hypoxia except for a significant increase in the antioxidant 2-oxoglutaric acid. This report firstly provides the holistic changes of various metabolic pathways of hypoxic cultured oral keratinocytes and fibroblasts.

Keywords: oxygen biology; metabolomics; oral keratinocytes; oral fibroblasts

1. Introduction

Oxygen plays an important role in energy metabolism and signal transduction in maintaining the homeostasis of the microenvironment of the living body. The response of cultured cells to oxygen concentration has attracted attention as a physiological factor. The partial pressure of oxygen (pO_2) varies throughout the body ranging from 9% pO_2 in the lungs to 0.1% pO_2 in the peripheral tissues, depending on blood flow. Mohyeldin et al. [1] reported that the oxygen concentration is >7% pO_2 in the dermis and 0.2–8% pO_2

in the epidermis. Skin appendages show lower oxygen concentrations than the epidermis; hair follicles have 0.1–0.8% pO_2 and sebaceous glands have 0.1–1.3% pO_2 [2,3]. Culturing keratinocytes at 2% oxygen concentration has been reported to suppress stratification, cellular enlargement, and differentiation [4]. In cultured fibroblasts, the production levels of vascular endothelial growth factor (VEGF) and type I collagen, which are related to angiogenesis, collagen production, and tissue remodeling, have been altered in hypoxic conditions, indicating their roles in tissue remodeling during wound healing [5]. Hypoxic conditions increase the induction efficiency of induced pluripotent stem (iPS) cells and promote the undifferentiated cell proliferation of mesenchymal stem cells and neural stem cells [6–8]; therefore, hypoxic cultures have been attempted to be applied in regenerative medicine.

Hypoxia-inducible factor 1-alpha (HIF-1a) is the main regulator of cellular hypoxic response and binds to promoters of genes encoding glucose transporters and glycolytic enzymes that are important for metabolic reprogramming from oxidative phosphorylation to glucose metabolism [3]. Decreased oxygen consumption in the mitochondria prevents the production of reactive oxygen species (ROS) by suppressing the electron transport system, resulting in cell survival under hypoxia [9]. In cancer tissues, energy production dominantly depends on the glycolysis pathway (Warburg Effect) [10], and various metabolic shifts, such as glutaminolysis activation, due to insufficient nutrition and oxygen have been observed [10].

Oral mucosa-derived cells are a useful source for regenerative medicine and basic research, including disease model fabrication [11]. The influence of oxygen concentrations on cancer and wound healing in oral mucosa has been examined [12,13]; however, no report on the oxygen concentration in vivo has been published. Since the culture of oral mucosal epithelial cells under hypoxic conditions suppresses differentiation and senescence and promotes colony formation, hypoxic exposure is beneficial for applications in regenerative medicine, similar to other cells [14].

Although metabolic reprogramming plays an important role in stem cell biology and pathological conditions under hypoxia, the effects of hypoxia on oral mucosal keratinocytes and fibroblasts are poorly elucidated. Therefore, the purpose of this study is to demonstrate the characteristics of the metabolic mechanisms of oral mucosal keratinocytes and fibroblasts in hypoxia.

2. Materials and Methods

2.1. Primary Cell Culture under Hypoxic Conditions

Primary human oral keratinocytes were isolated and cultured routinely in EpiLife® medium (Thermo Fisher Scientific, Waltham, MA, USA) supplemented with EpiLife® Defined Growth Supplements (Thermo Fisher Scientific), 0.06 mM Ca^{2+}, gentamicin (5.0 μg/mL; Thermo Fisher Scientific), and amphotericin B (0.375 μg/mL; Thermo Fisher Scientific) as described previously [15].

Primary oral fibroblast cultures were established by an explant culture technique using the connected tissue after the epithelial layer was scraped off. Small explants were placed in a 60-mm Petri dish (Corning, New York, NY, USA) and incubated in Dulbecco's modified Eagle medium (DMEM; FUJIFILM Wako Pure Chemical Corporation, Osaka, Japan) supplemented with 10% fetal bovine serum (Thermo Fisher Scientific), gentamicin, and amphotericin B as previously described [16].

Six of the oral mucosa keratinocytes and fibroblasts used in the study were from passages 3 to 5. To culture the cells under hypoxic conditions, culture vessels were placed in a humidified modular incubator chamber (Billups Rothenberg, Inc., Del Mar, CA, USA), flushed for 2 min with a gas mixture of either 2.0% O_2 (5.0% CO_2–93.0% N_2) or 0.5% O_2 (5.0% CO_2–94.5% N_2), and then placed in an incubator at 37°C. Cells were fed with either a 2% or a 0.5% O_2 tension equilibrating complete media every other day. As a normoxic condition (20% O_2), vessels were placed in ambient oxygen in an incubator at 37 °C with a humidified 5.0% CO_2 environment as described previously [17].

2.2. Metabolite Extraction

Oral keratinocytes and fibroblasts were plated on 100-mm dishes and cultured under 2% or 0.5% O_2 conditions for 24 h or 72 h. Each experimental condition was performed in duplicate for metabolite extraction and for cell counting after trypsinization to normalize the metabolomics data. For metabolite extraction, cells were washed twice with 5 mL of ice-cold 5% D-mannitol and then immersed in 1 mL of methanol containing internal standards (25 mM each of methionine sulfone, 2-[N-morpholino]-ethanesulfonic acid, and D-camphor-10-sulfonic acid) for 10 min on ice. The lysate was scraped and collected in 1.5 mL tubes, snap-frozen by liquid nitrogen, and then stored at −80 °C until analysis. To 400 µL of the dissolved samples, 400 µL of chloroform and 200 µL of Milli-Q water were added, and the mixture was centrifuged at 10,000× *g* for 3 min at 4 °C. The aqueous layer was filtered to remove large molecules by centrifugation through a 5-kDa cut-off filter (Merck Millipore, Burlington, MA, USA) at 9100× *g* for 2.0 h at 4 °C. Then, 320 µL of the filtrate was concentrated by centrifugation and dissolved in 50 µL of Milli-Q water containing reference compounds (200 µM each of 3-aminopyrrolidine and trimesate) immediately before the capillary electrophoresis time-of-flight mass spectrometry (CE-TOF-MS) analysis.

The instrumentation and measurement conditions used for CE-TOF-MS were described elsewhere [18]. Briefly, cations and anions in the 50–1000 m/z range were analyzed independently. The migration times of each chromatograph were normalized by dynamic programming-based methods, and metabolite identification was conducted by matching the m/z and corrected migration times with our standard library [19]. To calculate the absolute concentration of each metabolite, corresponding standard compounds were prepared. The peak area of each metabolite was divided by those of the internal standard compound (methionine sulfone) to calculate the relative area by eliminating the unexpected bias of MS sensitivity fluctuation. The standard mixture was measured before the sample measurement, and based on the ratio of relative areas of each metabolite in the sample and standard mixture, the concentrations were calculated. The upper and lower quantifications limits were already measured using standard mixtures, and the peaks under lower limits were treated as not detected (N.D.).

The overall metabolomic profiles were assessed by clustering analysis. Statistical analysis was performed by a two-tailed Student's *t*-test. Differences were considered significant at $p < 0.05$. The data processing and pathway visualization were conducted by our proprietary software, MasterHands and Pathway Visualization [19–21].

Frequently observed peaks (≥85% of all samples) were used for heatmap visualization and PCA. Pearson correlation was used for the metabolite alignment at heatmaps. These analysis and data visualizations were conducted using MetaboAnalyst (ver 5.0, https://www.metaboanalyst.ca/, acceded on 21 January 2021), GraphPad Prism (version 5.04, GraphPad Software, San Diego, CA, USA), and MeV TM4 software (version 4.9.0, http://mev.tm4.org/, acceded on 20 January 2021).

3. Results

3.1. The Metabolomic Concentration of Oral Keratinocytes and Oral Fibroblasts

Metabolomic analysis successfully identified and quantified 208 and 203 metabolites in cultured oral keratinocytes and fibroblasts, respectively, under atmospheric oxygen concentration. The $\log_2$ of fold change (F.C.) in the metabolite concentration between these cells and *p*-values are shown in the scatter plot (Figure 1). The 33 and 13 metabolites showed higher ($\log_2$ F.C. > 1) and lower ($\log_2$ F.C. < −1) concentration of keratinocytes at a significant level ($p < 0.05$), respectively.

PCA was performed individually for each cell type to evaluate the effect of oxygen concentrations. The score plots of keratinocyte revealed that the samples with normoxic conditions were located at the right (labeled as K 20%), 2% O_2 conditions were located at the center (K 2% 24 h and 72 h), and 0.5% O_2 conditions were located at the left (K 0.5% 24 h and 72 h) (Figure 2a). Thus, the first principal component (PC1) reflects the oxygen condition. The loading plots showed the distribution of various metabolites along with PC1.

Among amino acids, arginine (Arg), lysine (Lys), and threonine (Thr) showed a relatively small PC1 value (PC1 < −0.1), whereas the aspartate (Asp), asparagine (Asn), and alanine (Ala) showed larger PC1 values (PC > 0.15). Intermediate metabolites at tricarboxylic acid (TCA) cycles, such as citrate, succinate, fumarate, malate, and cis-aconitate also showed larger PC values (PC > 0.1).

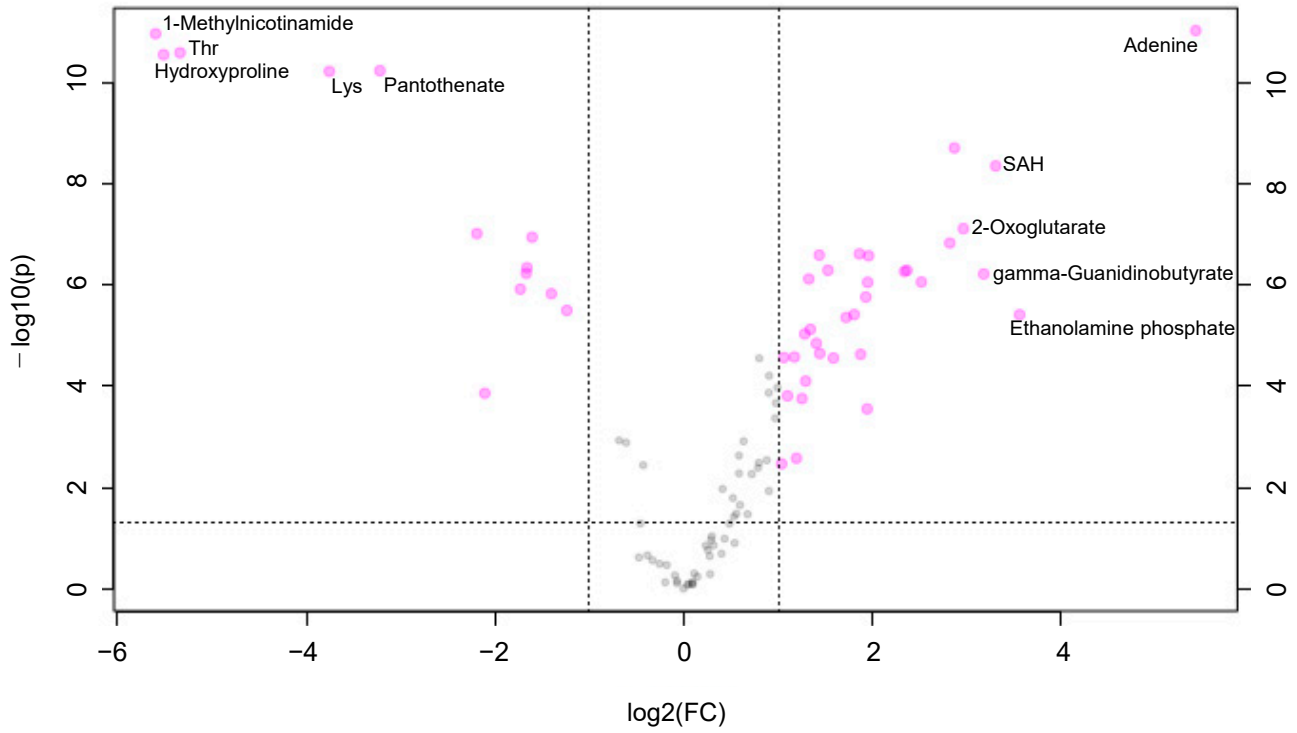

Figure 1. Volcano plots of the metabolomic profile. X-axis indicates the $\log_2$(fold change (F.C.)) of oral keratinocytes (n = 7)/fibroblasts cultured (n = 7) in a 20% oxygen environment. The Y-axis indicates $-\log_{10}$(P) using the t-test. Before the calculation of F.C., each metabolite concentration was divided by the average concentration of each sample to eliminate sample-dependent bias. Each plot indicates a metabolite. The metabolites showing a large difference in F.C. ($\log_2$(F.C.) < −1 or 1 < $\log_2$(F.C.)) and small p-value ($p < 0.05$) were colored in pink.

The score plots of fibroblast revealed that the samples with normoxic conditions (F 20%) were located at the upper left, the samples in 0.5% O_2 conditions for 72 h (F 0.5% 72 h) were located at the lower right vice versa, and the samples with other conditions were located between them (Figure 2b). Both PC1 and the second PC (PC2) reflect the difference in the oxygen used. The intermediate metabolites in glycolysis, such as glucose 1-phosphate (G1P), 3-phosphoglyceric acid (3PG), and phosphoenolpyruvate (PEP) are located at the lower right area. Oppositely, organic acids, such as succinate, isocitrate, malate, and fumarate were located in the upper left area.

The heatmaps of keratinocytes (Figure 2c) and fibroblasts (Figure 2d) show the F.C. of metabolite concentrations of each sample divided by those of the reference sample under atmospheric oxygen concentration, i.e., the red and blue colors indicate the relatively higher and lower concentration compared to the ones in the reference sample. Overall, the heatmap of keratinocytes showed clearer red and blue colors compared to one of the fibroblasts. Therefore, the metabolomic impact depending on the O_2 condition and culture duration of keratinocytes was more significant compared to the fibroblasts. In both samples, the number of metabolites showing higher concentration was fewer than the number of metabolites showing lower concentration. Only sedoheptulose 7-phosphate (S7P), an intermediate metabolite in the pentose phosphate pathway (PPP), showed significantly higher ($p < 0.05$) compared to the reference samples in any culture condition in both samples (Figure 2c,d and Figure 3).

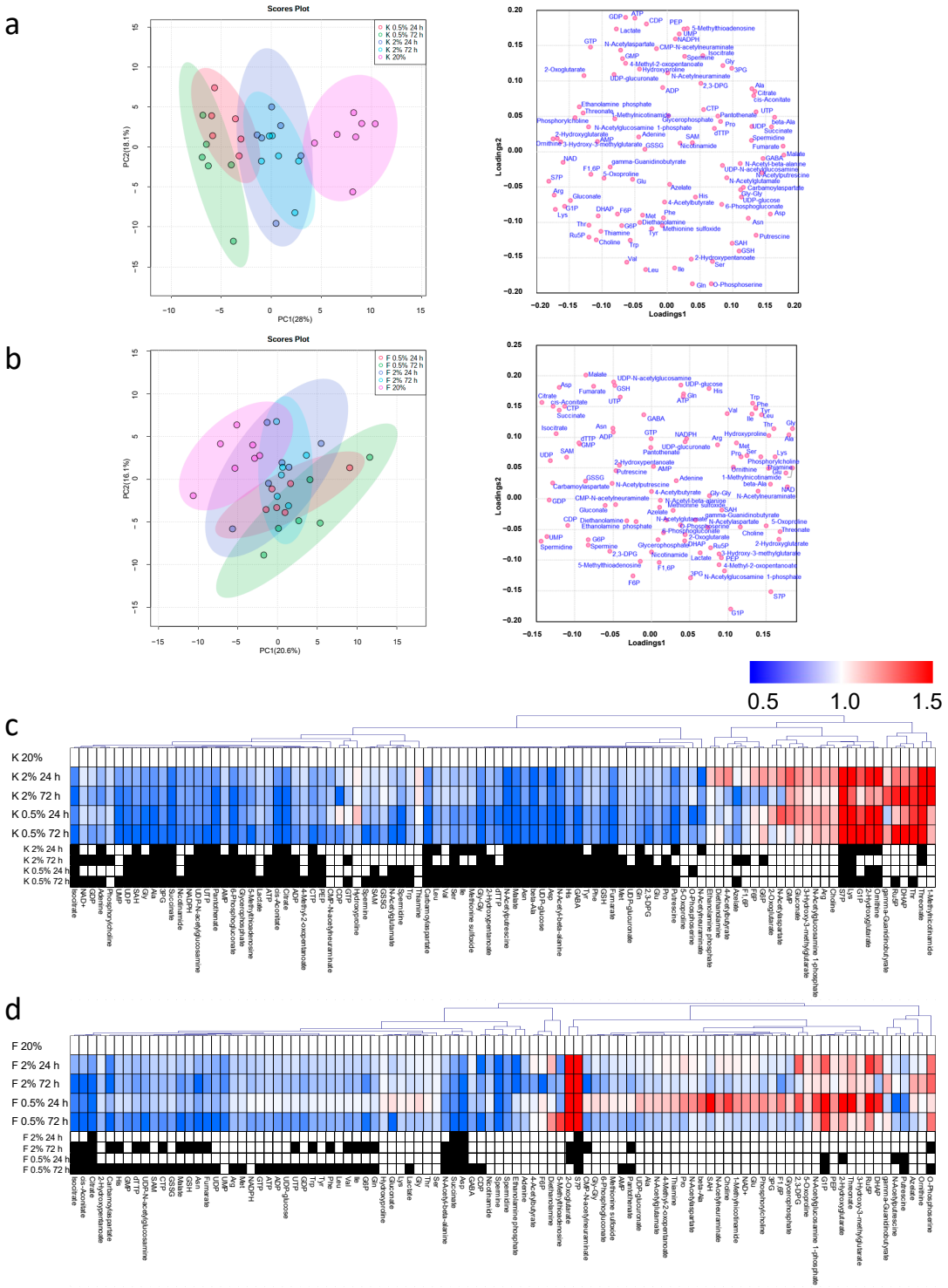

Figure 2. Principal component analyses (PC) of keratinocytes (**a**) and fibroblasts (**b**). The left and right panels were score plots and loading plots, respectively. The X and Y-axes indicated the first and the second PC with contribution ratios. Each plot indicates sample and metabolites in score and loading plots, respectively. Each metabolite concentration was divided by the sum of all metabolite concentrations of each sample, transformed to $\log_2$ and Z-score before PC analysis. Heatmap of keratinocytes (**c**) and fibroblasts (**d**). Each box in the heatmap indicated the fold change (F.C.); i.e., the averaged values of metabolite concentrations of each sample were divided by those of the reference samples cultured under 20% O_2. The color bar indicated F.C. The black boxes indicated $p < 0.05$ (Student's t-test) between each sample and the reference sample. The cells were cultured under the condition with 20% O_2 ($n = 7$), 2% O_2 for 24 h ($n = 6$), 2% O_2 for 72 h ($n = 6$), 0.5% O_2 for 24 h ($n = 6$), and 0.5% O_2 for 72 h ($n = 6$).

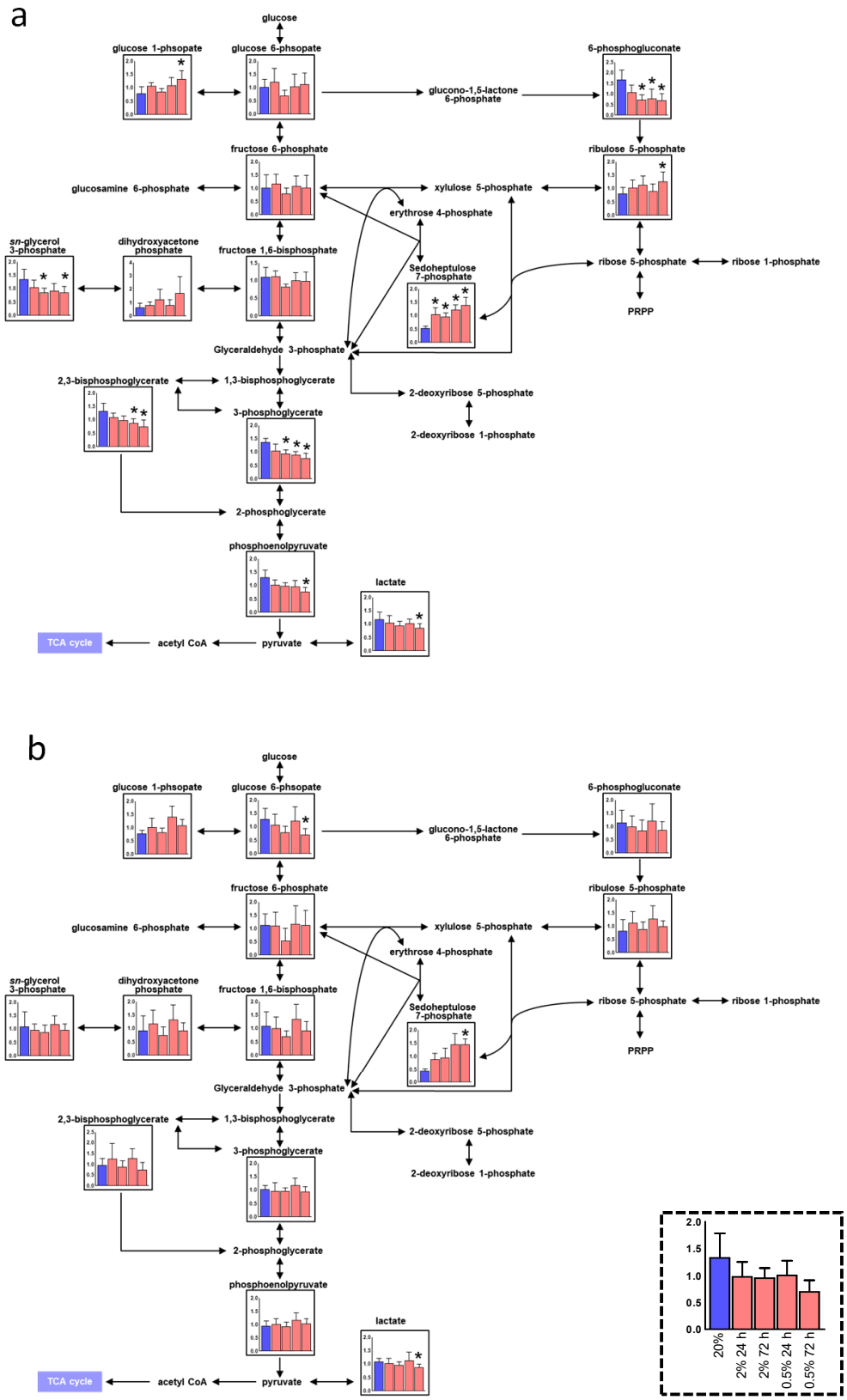

Figure 3. Metabolic pathways of glycolysis and pentose phosphate pathway (PPP) of oral keratinocytes (**a**) and oral fibroblasts (**b**) in hypoxic culture (n = 6). Quantified metabolite concentrations are shown as bars; ambient oxygen cultured (blue), 2% O_2 for 24 h, 2% O_2 for 72 h, 0.5% O_2 for 24 h, and 0.5% O_2 for 72 h from the left, respectively. p-values were calculated using Student's t-test (two-tailed, unequal variance). * $p < 0.05$ was shown for comparison between each data with data for 20% oxygen.

3.2. Alteration of the Pentose Phosphate Pathway (PPP) and Urea Cycle under Hypoxia

Among various metabolic pathways, the PPP and urea cycle with various ambient oxygen cultures showed a distinct difference between oral keratinocytes and fibroblasts (Figures 3 and 4). Among the 13 metabolites in the PPP, 11 and three showed significant differences depending on the O_2 condition in oral keratinocytes and oral fibroblasts, respectively (Figure 3). In the urea cycles, including 22 metabolites, 11 and two metabolites showed a significant difference in these cells (Figure 4). Time dependency in 2% O_2 showed less difference comparing with that of 0.5%. As commonly observed features in both cells, lactate, an end product of glycolysis, decreased significantly in 0.5% 72 h (Figure 3a,b). 6-phosphogluconate (6PG) showed a significant decrease, whereas ribose 5-phosphate (R5P), the intermediate metabolites in PPP, significantly increased in the hypoxic oral keratinocytes. A decrease of phosphoribosyl pyrophosphate synthetase1 and 2 (PRPS1 and 2), ribose 5-phosphate isomerase A (RPIA), and ribulose-5-phosphate-3-epimerase (RPE) were observed, which may lead to the accumulation of R5P by producing less PRPP and xylose-5P. Oral fibroblasts showed a decrease of glucose 6-phosphate (G6P) in hypoxia, while oral keratinocytes did not. According to our microarray results, glucose 6-phosphate isomerase (GPI), which is needed to convert G6P to F6P, was higher in hypoxic oral fibroblasts (Table S1). In addition, the NADPH/NADP+ ratio regulates the activity of glucose 6-phosphate dehydrogenase (GPD), which converts G6P to D-Glucono-1,5-lactone 6-phosphate; the latter has a lower tendency in hypoxic oral fibroblasts (data not shown [22]), which may also contribute to the low level of G6P [23]. G6P in oral fibroblasts showed the same tendency with 6PG which indicates the constant metabolism kinetics between them.

Interestingly, oral keratinocytes and fibroblasts showed unique balance changes among intermediate metabolites in the urea cycle and polyamines. Reduced Asn in both hypoxic cells may be because of the decrease of glutamic-oxaloacetic transaminase 1 (GOT1) gene expression level, which generates Asn under hypoxia (Table S1) [24]. Increased 2-oxoglutaric acid (α-ketoglutaric acid; α-KG) was observed in hypoxic oral fibroblasts. Glutamine (Glu), Asn, and fumarate are decreased in both hypoxic cells while ornithine increased in hypoxic oral keratinocytes and did not decrease in hypoxic oral fibroblasts. The decrease of argininosuccinate synthase 1 (ASS1) is consistent with the low level of argininosuccinate in both hypoxic cells (Table S1). Ornithine is catabolized by ornithine decarboxylase 1 (ODC1) to putrescine as a substrate for the synthesis of polyamines, such as spermidine and spermine. As a result of the decrease of ODC1, putrescine and other polyamines (i.e., spermidine, spermine, and acetyl-putrescine) may decrease in contrast to ornithine in both hypoxic cells (Figure 4a,b, Table S1).

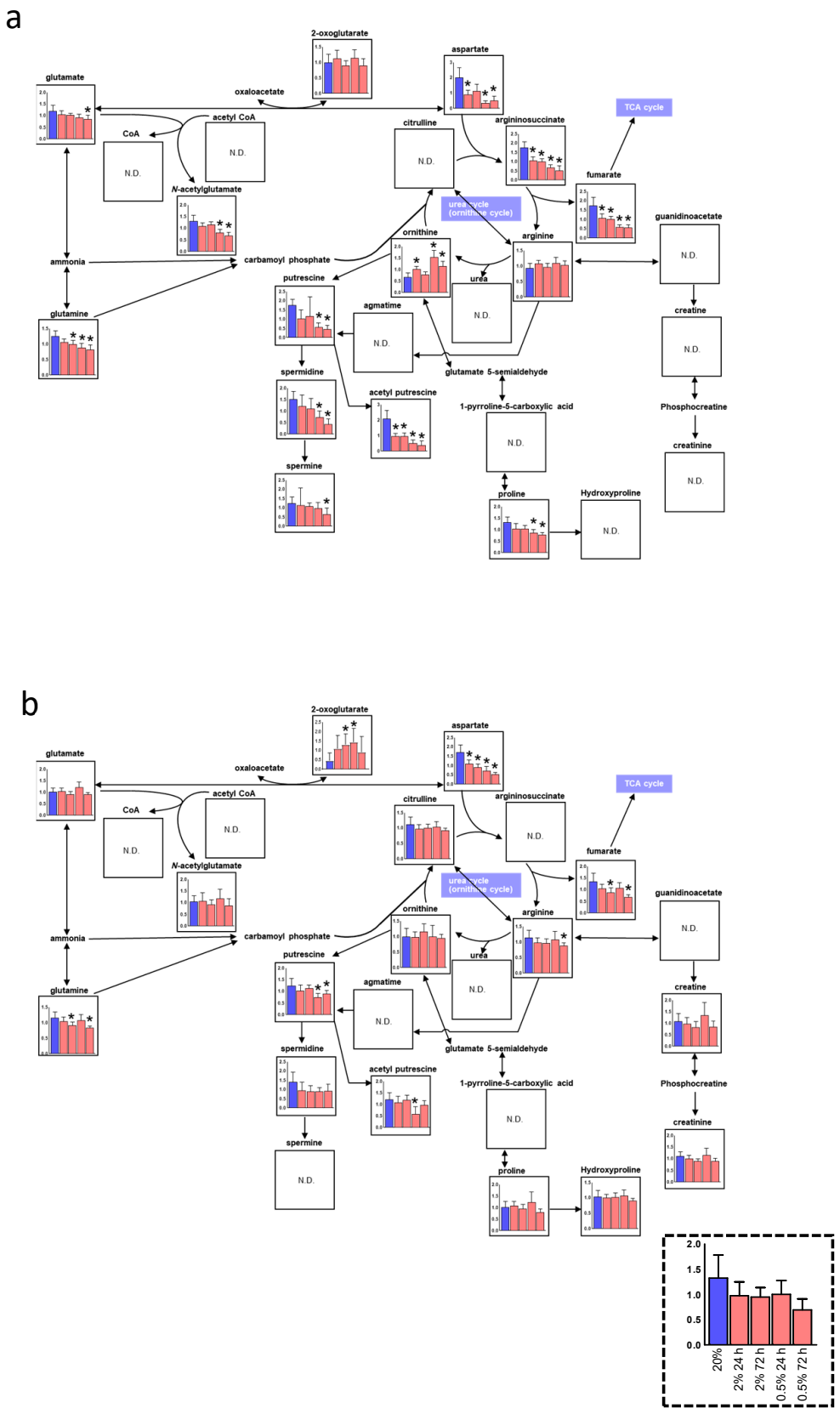

Figure 4. Metabolic pathway maps of the urea cycle of oral keratinocytes (**a**) and oral fibroblasts (**b**) in hypoxic culture (n = 6). Quantified metabolite concentrations are shown as bars; ambient oxygen cultured (blue), 2% O_2 for 24 h, 2% O_2 for 72 h, 0.5% O_2 for 24 h, and 0.5% O_2 for 72 h, from left, respectively. p-values were calculated using Student's t-test (two-tailed, unequal variance). * $p < 0.05$ was shown for comparison between each data for 20% oxygen.

4. Discussion

Keratinocytes in the stratified squamous epithelium are the major cellular components of the oral mucosa, which are derived from the ectoderm. Fibroblasts in the fibrous connective tissue layer are derived from the mesoderm. Although they are adjacent tissues to the border of the basement membrane, their cellular characteristics vary because of their origin. Since metabolic conditions under the hypoxic microenvironment of their cells are supposed to be further different from the ambient condition, we conducted metabolomic analyses in various oxygen conditions to characterize their metabolomic features.

Oral keratinocytes and fibroblasts under atmospheric oxygen concentration showed the presence of various metabolites with different concentrations. In oral fibroblasts, lysine and ornithine, which are required for collagen synthesis and crosslinking, were higher [25,26]. In contrast, *N*-acetylputrescine, one of the polyamine metabolites important for maintaining epithelial homeostasis, was higher in oral keratinocytes [27]. Thus, metabolites of oral keratinocytes are quite distinct from those of oral fibroblasts even under 20% oxygen concentration.

Metabolomic analyses were conducted under two different environmental factors, exposure time and oxygen concentrations. The cells were exposed for either 24 (short-term) or 72 h (long-term) and then cultured in 2% oxygen, which is the concentration preferred by keratinocyte precursor cells, as well as 0.5% oxygen, which is a severe oxygen concentration, such as in wound healing. Oral keratinocytes showed various metabolic changes in response to hypoxia, especially in glycolysis, the PPP, and the urea cycle. In a temporal metabolomic analysis of the first-line response to oxidative stress, it has been reported that epidermal keratinocytes and dermal fibroblasts showed fluctuation in glycolysis and PPP metabolites within 1 min [28]. Differences in time dependency were little, especially in 2% O_2, which may be because the time course was excessive in the present study.

In hematopoietic and pluripotent stem cells, PPP was elevated [29,30]. Glycolysis and PPP dominantly produce energy and suppress the generation of ROS, which is an important mediator of cell damage and the cell death process, and it maintains the quiescent state as well. We previously reported that ROS generation was suppressed under hypoxia in oral keratinocytes [14]. Nonetheless, the proliferation of oral keratinocytes increased at 2% and 0.5% oxygen concentrations [14]. A decrease of G6P was seen in hypoxic oral fibroblasts. The upregulation of GPI and downregulation of NADPH/NADP+ that are reported as the hypoxic reaction may retrieve cellular survival and increase proliferation and angiogenesis in hypoxic oral fibroblasts [23,31]. This study revealed that the production of R5P, which is the intermediate metabolite of PPP, increased while 6PG decreased in hypoxic oral keratinocytes. Gene expression changes of 6-phosphogluconate dehydratase (PGD), which produces 6PG from R5P, and transaldolase1 (TALDO1), which produces erythrose 4-phosphate (E4P) and fructose 6-phosphate (F6P) from S7P and glyceraldehyde 3-phosphate (G3P) were inconsistent with their related metabolite changes (Figure 3, Table S1). The activity of PGD and TALDO increases sharply in alkaline pH [32,33], which may lead to low 6PG synthesis or high S7P, since the intracellular environment of hypoxic cells is acidic [34]. 6-phosphofructo-2-kinase/fructose-2,6-biphosphatase 3 (PFKFB3) is an enzyme that switches glycolysis to PPP, and it was elevated in both hypoxic cells (Table S1). It could maintain oral keratinocytes in an undifferentiated state in conjunction with p63, an undifferentiated marker of keratinocytes, and promote collagen synthesis in oral fibroblasts [35,36].

The various metabolites' concentration in the polyamine pathway and the aspartate to fumarate in the urea cycle were reduced, and the accumulation of ornithine was also found in both hypoxic cell types. The limitation of Asn supports cellular proliferation in hypoxic cancer, which is consistent with our previous study that oral keratinocytes highly proliferate in hypoxia [24,37,38]. Mitochondrial activity is low in hypoxia; as a result, fumarate synthesis decreased following the whole TCA cycle deactivation [39]. A low level of polyamines was observed in both hypoxic cell types. Since polyamines are

known to be involved in the keratinocyte cell differentiation process [40], the result in this study was consistent with our previous study that showed that hypoxia maintained an undifferentiated state of oral keratinocytes.

In contrast to oral keratinocytes, oral fibroblasts demonstrated fewer changes in both the PPP and urea cycle. Oral fibroblasts showed the deactivation of overall metabolism, particularly, the metabolites of the TCA cycle, which was lower than those in oral keratinocytes. In addition, both the PPP and the urea cycle in oral fibroblasts are less susceptible to hypoxia than those in oral keratinocytes. In contrast, an increase in α-KG, which is a co-activator of prolyl hydroxylase that is an HIF-1a degrading enzyme, was observed under hypoxia. α-KG, an endogenous intermediate metabolite in the TCA cycle, is a molecule that is involved in multiple metabolic and cellular pathways as well as acting as an antioxidant [41]. Therefore, in oral fibroblasts, α-KG inhibits ROS in hypoxia, which may be involved in cell survival and cellular senescence.

The present study has several limitations. First, we used a limited number of samples because of the usage of primary culture cells. Second, we did not perform any functional assays. By clarifying the molecular response of this metabolic reprogramming, further studies on cellular hypoxic responses are necessary in the future. Focusing on subcellular compartments of glutamine metabolism and its lipogenesis might reveal novel functions [42,43]. Here, we discussed the expression of the metabolic enzymes using only microarray data. Validation of these expressions and activities is required to confirm the reason for metabolomic pathways' change.

In conclusion, we observed the metabolomic concentrations of oral keratinocytes and fibroblasts for the first time and revealed their holistic changes of two major cell types in the oral mucosa. An increase in PPP and a decrease in polyamine production under hypoxia were detected in this study, which would support our previous data showing that hypoxia can maintain oral keratinocytes in an undifferentiated state and prevent them from cellular senescence. In oral fibroblasts, the overall metabolism changes were smaller than those of oral keratinocytes. Although there were only little changes in any pathway under hypoxia, the concentration of α-KG increased. The metabolic reprogramming findings of our study could contribute to providing insights into stem cell biology, wound healing, and cancer biology.

Supplementary Materials: The following are available online at https://www.mdpi.com/2077-0383/10/6/1156/s1, Table S1: DNA microarray analysis.

Author Contributions: H.K. contributed to the conception, design, data acquisition, analysis, and interpretation drafted; M.S. contributed to the conception, data analysis, and interpretation, drafted; A.E. and M.K. contributed to data acquisition and analysis; Y.H., N.S. and A.S. contributed to data acquisition; H.O. contributed to interpretation; K.I. contributed to the conception, design, and interpretation. All authors have read and agreed to the published version of the manuscript.

Funding: This work was supported by a Grant-in-Aid for Scientific Research to H.K. (No. 15K20476), M.S. (No. 20B205), and to H.O. (No. 17K11800) and the grants from Yamagata Prefecture and Tsuruoka City to M.S.

Institutional Review Board Statement: All procedures performed in studies involving human participants were following the ethical standards of the institutional and/or national research committee and with the 1964 Helsinki declaration and its later amendments or comparable ethical standards. The protocol for obtaining human keratinized oral mucosa tissue samples was approved by the Niigata University Hospital Internal Review Board (2015–5018).

Informed Consent Statement: Patients undergoing minor dentoalveolar surgery were provided sufficient information regarding this study, and all participating individuals signed an informed consent form.

Data Availability Statement: The data presented in this study are available on request from the corresponding author. The data are not publicly available.

Conflicts of Interest: Authors declare that they have no conflict of interest.

References

1. Mohyeldin, A.; Garzón-Muvdi, T.; Quiñones-Hinojosa, A. Oxygen in Stem Cell Biology: A Critical Component of the Stem Cell Niche. *Cell Stem Cell* **2010**, *7*, 150–161. [CrossRef]
2. Evans, S.M.; Schrlau, A.E.; Chalian, A.A.; Zhang, P.; Koch, C.J. Oxygen levels in normal and previously irradiated human skin as as-sessed by EF5 binding. *J. Investig. Dermatol.* **2006**, *126*, 2596–2606. [CrossRef]
3. Rezvani, H.R.; Ali, N.; Serrano-Sanchez, M.; Dubus, P.; Varon, C.; Ged, C.; Pain, C.; Cario-André, M.; Seneschal, J.; Taïeb, A.; et al. Loss of epidermal hypoxia-inducible factor-1α accelerates epidermal aging and affects re-epithelialization in human and mouse. *J. Cell Sci.* **2011**, *124*, 4172–4183. [CrossRef]
4. Ngo, M.A.; Sinitsyna, N.N.; Qin, Q.; Rice, R.H. Oxygen-Dependent Differentiation of Human Keratinocytes. *J. Investig. Dermatol.* **2007**, *127*, 354–361. [CrossRef]
5. Steinbrech, D.S.; Longaker, M.T.; Mehrara, B.J.; Saadeh, P.B.; Chin, G.S.; Gerrets, R.P.; Chau, D.C.; Rowe, N.M.; Gittes, G.K. Fibroblast response to hypoxia: The relationship between angio-genesis and matrix regulation. *J. Surg. Res.* **1999**, *84*, 127–133. [CrossRef]
6. Yoshida, Y.; Takahashi, K.; Okita, K.; Ichisaka, T.; Yamanaka, S. Hypoxia Enhances the Generation of Induced Pluripotent Stem Cells. *Cell Stem Cell* **2009**, *5*, 237–241. [CrossRef]
7. Santilli, G.; Lamorte, G.; Carlessi, L.; Ferrari, D.; Nodari, L.R.; Binda, E.; Delia, D.; Vescovi, A.L.; De Filippis, L. Mild Hypoxia Enhances Proliferation and Multipotency of Human Neural Stem Cells. *PLoS ONE* **2010**, *5*, e8575. [CrossRef] [PubMed]
8. Yamamoto, Y.; Fujita, M.; Tanaka, Y.; Kojima, I.; Kanatani, Y.; Ishihara, M.; Tachibana, S. Low oxygen tension enhances proliferation and maintains stemness of ad-ipose tissue-derived stromal cells. *Biores. Open Access* **2013**, *2*, 199–205. [CrossRef] [PubMed]
9. Goda, N.; Kanai, M. Hypoxia-inducible factors and their roles in energy metabolism. *Int. J. Hematol.* **2012**, *95*, 457–463. [CrossRef] [PubMed]
10. Altman, B.J.; Stine, Z.E.; Dang, B.J.A.Z.E.S.C.V. From Krebs to clinic: Glutamine metabolism to cancer therapy. *Nat. Rev. Cancer* **2016**, *16*, 619–634. [CrossRef]
11. Izumi, K.; Kato, H.; Feinberg, S.E. Three-dimensional reconstruction of oral mucosa. In *Tissue Engineering Strategies. Stem Cell Biology and Tissue Engineering in Dental Science*; Vishwakarma, A., Sharpe, P., Shi, S., Wang, X.-P., Ramalingam, M., Eds.; Academic Press/Elsevier: Waltham, MA, USA, 2015; Chapter 53, pp. 721–731.
12. Thorn, J.J.; Kallehave, F.; Westergaard, P.; Hansen, E.H.; Gottrup, F. The effect of hyperbaric oxygen on irradiated oral tissues: Transmuco-sal oxygen tension measurements. *J. Oral Maxillofac. Surg.* **1997**, *55*, 1103–1107. [CrossRef]
13. Chen, L.; Gajendrareddy, P.K.; DiPietro, L.A. Differential Expression of HIF-1α in Skin and Mucosal Wounds. *J. Dent. Res.* **2012**, *91*, 871–876. [CrossRef]
14. Kato, H.; Izumi, K.; Uenoyama, A.; Shiomi, A.; Kuo, S.; Feinberg, S.E. Hypoxia induces an undifferentiated phenotype of oral keratinocytes in vitro. *Cells Tissues Organs* **2014**, *199*, 393–404. [CrossRef] [PubMed]
15. Kato, H.; Izumi, K.; Saito, T.; Ohnuki, H.; Terada, M.; Kawano, Y.; Nozawa-Inoue, K.; Saito, C.; Maeda, T. Distinct expression patterns and roles of aldehyde dehydrogenases in normal oral mucosa keratinocytes: Differential inhibitory effects of a pharma-cological inhibitor and RNAi-mediated knockdown on cellu-lar phenotype and epithelial morphology. *Histochem. Cell Biol.* **2013**, *139*, 847–862. [CrossRef] [PubMed]
16. Uenoyama, A.; Kakizaki, I.; Shiomi, A.; Saito, N.; Hara, Y.; Saito, T.; Ohnuki, H.; Kato, H.; Takagi, R.; Maeda, T.; et al. Effects of C-xylopyranoside derivative on epithelial regeneration in an in vitro 3D oral mucosa model. *Biosci. Biotechnol. Biochem.* **2016**, *80*, 1344–1355. [CrossRef]
17. Kato, H.; Marcelo, C.L.; Washington, J.B.; Bingham, E.L.; Feinberg, S.E. Fabrication of Large Size Ex Vivo-Produced Oral Mucosal Equivalents for Clinical Application. *Tissue Eng. Part C Methods* **2015**, *21*, 872–880. [CrossRef] [PubMed]
18. Sakagami, H.; Sugimoto, M.; Kanda, Y.; Murakami, Y.; Amano, O.; Saitoh, J.; Kochi, A. Changes in Metabolic Profiles of Human Oral Cells by Benzylidene Ascorbates and Eugenol. *Medicines* **2018**, *5*, 116. [CrossRef] [PubMed]
19. Sugimoto, M.; Sakagami, H.; Yokote, Y.; Onuma, H.; Kaneko, M.; Mori, M.; Sakaguchi, Y.; Soga, T.; Tomita, M. Non-targeted metabolite profiling in activated macrophage secretion. *Metabolomics* **2011**, *8*, 624–633. [CrossRef]
20. Sugimoto, M.; Wong, D.T.; Hirayama, A.; Soga, T.; Tomita, M. Capillary electrophoresis mass spectrometry-based saliva metabolomics identified oral, breast and pancreatic cancer-specific profiles. *Metabolomics* **2009**, *6*, 78–95. [CrossRef]
21. Sugimoto, M. Metabolomic pathway visualization tool outsourcing editing function. In Proceedings of the 2015 37th Annual International Conference of the IEEE Engineering in Medicine and Biology Society (EMBC), Milan, Italy, 25–29 August 2015; Volume 2015, pp. 7659–7662.
22. Kato, H. Niigata University, Niigata, Japan. Unpublished work, 2021.
23. Semenza, G.L. Hypoxia-inducible factors: Coupling glucose metabolism and redox regulation with induction of the breast cancer stem cell phenotype. *EMBO J.* **2017**, *36*, 252–259. [CrossRef]
24. Meléndez-Rodríguez, F.; Urrutia, A.A.; Lorendeau, D.; Rinaldi, G.; Roche, O.; Böğürcü-Seidel, N.; Muelas, M.O.; Mesa-Ciller, C.; Turiel, G.; Bouthelier, A.; et al. HIF1α Suppresses Tumor Cell Proliferation through Inhi-bition of Aspartate Biosynthesis. *Cell Rep.* **2019**, *26*, 2257–2265. [CrossRef] [PubMed]
25. Shi, H.P.; Fishel, R.S.; Efron, D.T.; Williams, J.Z.; Fishel, M.H.; Barbul, A. Effect of Supplemental Ornithine on Wound Healing. *J. Surg. Res.* **2002**, *106*, 299–302. [CrossRef] [PubMed]
26. Yamauchi, M.; Sricholpech, M. Lysine post-translational modifications of collagen. *Essays Biochem.* **2012**, *52*, 113–133. [CrossRef]

27. Roseeuw, D.I.; Marcelo, C.L.; Rhodes, L.M.; Voorhees, J.J. Epidermal keratinocytes actively maintain their intracellular polyamine levels. *Cell Tissue Kinet.* **1983**, *16*, 493–504. [PubMed]
28. Kuehne, A.; Emmert, H.; Soehle, J.; Winnefeld, M.; Fischer, F.; Wenck, H.; Gallinat, S.; Terstegen, L.; Lucius, R.; Hildebrand, J.; et al. Acute Activation of Oxidative Pentose Phosphate Pathway as First-Line Response to Oxidative Stress in Human Skin Cells. *Mol. Cell* **2015**, *59*, 359–371. [CrossRef] [PubMed]
29. Takubo, K.; Nagamatsu, G.; Kobayashi, C.I.; Nakamura-Ishizu, A.; Kobayashi, H.; Ikeda, E.; Goda, N.; Rahimi, Y.; Johnson, R.S.; Soga, T.; et al. Regulation of Glycolysis by Pdk Functions as a Metabolic Checkpoint for Cell Cycle Quiescence in Hematopoietic Stem Cells. *Cell Stem Cell* **2013**, *12*, 49–61. [CrossRef]
30. Hawkins, K.E.; Joy, S.; Delhove, J.M.; Kotiadis, V.N.; Fernandez, E.; Fitzpatrick, L.M.; Whiteford, J.R.; King, P.J.; Bolanos, J.P.; Duchen, M.R.; et al. NRF2 Orchestrates the Metabolic Shift during Induced Pluripotent Stem Cell Reprogramming. *Cell Rep.* **2016**, *14*, 1883–1891. [CrossRef] [PubMed]
31. Lu, Y.; Yu, S.-S.; Zong, M.; Fan, S.-S.; Lu, T.-B.; Gong, R.-H.; Sun, L.-S.; Fan, L.-Y. Glucose-6-Phosphate Isomerase (G6PI) Mediates Hypoxia-Induced Angiogenesis in Rheumatoid Arthritis. *Sci. Rep.* **2017**, *7*, 40274. [CrossRef] [PubMed]
32. Pavlides, S.; Whitaker-Menezes, D.; Castello-Cros, R.; Flomenberg, N.; Witkiewicz, A.K.; Frank, P.G.; Casimiro, M.C.; Wang, C.; Fortina, P.; Addya, S.; et al. The reverse Warburg effect: Aerobic glycolysis in cancer associated fibroblasts and the tumor stroma. *Cell Cycle* **2009**, *8*, 3984–4001. [CrossRef]
33. Alfarouk, K.O.; Ahmed, S.; Elliott, R.L.; Benoit, A.; Alqahtani, S.S.; Ibrahim, M.E.; Bashir, A.H.H.; Alhoufie, S.T.S.; Elhassan, G.O.; Wales, C.C.; et al. The pentose phosphate pathway dynamics in cancer and its de-pendency on intracellular pH. *Metabolites* **2020**, *10*, 285. [CrossRef]
34. Sørensen, B.S.; Busk, M.; Overgaard, J.; Horsman, M.R.; Alsner, J. Simultaneous hypoxia and low extracellular pH suppress overall metabol-ic rate and protein synthesis in vitro. *PLoS ONE* **2015**, *10*, 1–14. [CrossRef]
35. Hamanaka, R.B.; Mutlu, G.M. PFKFB3, a Direct Target of p63, Is Required for Proliferation and Inhibits Differentiation in Epidermal Keratinocytes. *J. Investig. Dermatol.* **2017**, *137*, 1267–1276. [CrossRef] [PubMed]
36. Hu, X.; Xu, Q.; Wan, H.; Hu, Y.; Xing, S.; Yang, H.; Gao, Y.; He, Z. PI3K-Akt-mTOR/PFKFB3 pathway mediated lung fibroblast aerobic glycolysis and col-lagen synthesis in lipopolysaccharide-induced pulmonary fibrosis. *Lab. Investig.* **2020**, *100*, 801–811. [CrossRef] [PubMed]
37. Sullivan, L.B.; Luengo, A.; Danai, L.V.; Bush, L.N.; Diehl, F.F.; Hosios, A.M.; Lau, A.N.; Elmiligy, S.; Malstrom, S.; Lewis, C.A.; et al. Aspartate is an endogenous metabolic limitation for tumour growth. *Nat. Cell Biol.* **2018**, *20*, 782–788. [CrossRef] [PubMed]
38. Garcia-Bermudez, J.; Baudrier, L.; La, K.; Zhu, X.G.; Fidelin, J.; Sviderskiy, V.O.; Papagiannakopoulos, T.; Molina, H.; Snuderl, M.; Lewis, C.A.; et al. Aspartate is a limiting metabolite for cancer cell proliferation under hy-poxia and in tumours. *Nat. Cell Biol.* **2018**, *20*, 775–781. [CrossRef]
39. Lee, P.; Chandel, N.S.; Simon, M.C. Cellular adaptation to hypoxia through hypoxia inducible factors and beyond. *Nat. Rev. Mol. Cell Biol.* **2020**, *21*, 268–283. [CrossRef]
40. Pietilä, M.; Pirinen, E.; Keskitalo, S.; Juutinen, S.; Pasonen-Seppänen, S.; Keinänen, T.; Alhonen, L.; Jänne, J. Disturbed keratinocyte differentiation in transgenic mice and organotypic keratinocyte cultures as a result of spermidme/spermine N1-acetyltransferase overexpression. *J. Investig. Dermatol.* **2005**, *124*, 596–601. [CrossRef]
41. Zdzisińska, B.; Żurek, A.; Kandefer-Szerszeń, M. Alpha-Ketoglutarate as a Molecule with Pleiotropic Activity: Well-Known and Novel Possibilities of Therapeutic Use. *Arch. Immunol. Ther. Exp.* **2017**, *65*, 21–36. [CrossRef]
42. Lee, W.D.; Mukha, D.; Aizenshtein, E.; Shlomi, T. Spatial-fluxomics provides a subcellular-compartmentalized view of reductive glutamine metabolism in cancer cells. *Nat. Commun.* **2019**, *10*, 1–14. [CrossRef]
43. Wang, Y.; Bai, C.; Ruan, Y.; Liu, M.; Chu, Q.; Qiu, L.; Yang, C.; Li, B. Coordinative metabolism of glutamine carbon and nitrogen in proliferating cancer cells under hypoxia. *Nat. Commun.* **2019**, *10*, 1–14. [CrossRef]